ISBN: 978-3-95450-236-3 ISSN: 2673-7027 doi:10.18429/JACoW-eeFACT2022-WEXAS0102

SuperKEKB OPERATING EXPERIENCE OF RF SYSTEM AT HIGH CURRENT

M. Nishiwaki*, T. Abe, K. Akai, S. Enomoto, T. Furuya, A. Kabe, T. Kageyama, T. Kobayashi, K. Marutsuka, S. Mitsunobu, Y. Morita, K. Nakanishi, S. Ogasawara, T. Okada, M. Ono, H. Sakai, Y. Takeuchi, K. Watanabe, M. Yoshida, S. Yoshimoto and K. Yoshino
High Energy Accelerator Research Organization (KEK), Tsukuba, Japan

Abstract

SuperKEKB aims for high luminosity on the order of 10^{35} /cm^2/s with high beam currents of 2.6 A for electron and 3.6 A for positron to search a new physics beyond the Standard Model in the B meson regime. In recent operations, we achieved new record of the luminosity of 4.7×10^{34} /cm^2/s with 1.1 A for electron and 1.3 A for positron. The RF system that is basically reused from KEKB is operating stably in the high current operation owing to the measures against to large beam power and HOM power. To cope with the large beam power, it has been increased the number of klystrons that drive only one normal conducting cavity (ARES) and reinforced the input couplers of ARES. As a measure against HOM power, the additional HOM dampers have been installed to superconducting cavities. One-third of LLRF control systems have been replaced with newly developed digital system to improve accuracy and flexibility. New damper system for coupled bunch instability expected in high current has been installed to new digital system. In this report, operation status of RF system under the high current operation will be presented.

INTRODUCTION

The SuperKEKB accelerator that is an electron-positron asymmetric energy collider is an upgrade machine from KEKB accelerator aiming for a significant increase of luminosity. SuperKEKB main ring consists of a 7 GeV electron ring (high energy ring, HER) and a 4 GeV positron ring (low energy ring, LER). To achieve high luminosity, the beam currents are designed as 2.6 A for HER and 3.6 A for LER [1]. The first commissioning beam operation without collision was performed in 2016 as Phase-1. After the Belle II detector rolled in, Phase-2 beam operation started and the first beam collision event was observed at Belle II in 2018. A full-scale collision experiment (Phase-3) has been continued since 2019. In recent operation, the achieved beam currents are 1.14 A for HER and 1.46 A for LER, and the peak luminosity of 4.65×10^{34} /cm^2/s was recorded [2, 3].

The RF-related operation parameters in KEKB (achieved) and SuperKEKB (design) are shown in Table 1. The design beam current is nearly twice as high as the KEKB achieved, and the beam power becomes large accordingly [4–6]. The RF system consisting both of normal-conducting cavities (ARES) [7–9] and superconducting cavities (SCC) [10, 11] has been reused from KEKB with reinforcement to handle the high beam current and the large beam power. The ARES stations have 1:2 configuration in which one klystron drives two ARESs, and 1:1 configuration in which one klystron drives one ARES. The SCC station has one cavity driven by one klystron.

The main upgrade items are as follows:

- Increasing the number of RF klystron stations of ARES 1:1 configuration.
- In ARES, changing input coupling factor β from 3 (1:2 configuration) to 5 (1:1 configuration).
- In SCC, installation of additional higher-order-mode (HOM) dampers.
- In High-Power RF (HPRF) system, replacement of deteriorated klystrons with higher gain and more stable ones.
- In Low-Level RF (LLRF) system, replacing with new digital LLRF system in a part of ARES 1:1 stations and development of new damper system for coupled instability.

The addition of klystron to upgrade from ARES 1:2 to 1:1 configuration and the increase of input coupling factor of ARES are essential to provide the large beam power. The HOM power excited in the SCC module at the design current is estimated to be more than double the power achieved in KEKB, and to exceed the allowable power of the existing ferrite dampers. Then, additional dampers are necessary to reduce the load of ferrite dampers. The replacement of the old HPRF and LLRF systems with new systems increases the stability and accuracy of beam operation.

The layout of RF stations in SuperKEKB at present is shown in Fig. 1. There are a total of 30 RF klystron stations consisting 16 ARES (22 cavities) stations in LER and 6 ARES (8 cavities) and 8 SCC stations in HER. To date, the number of ARES 1:1 station is partially increased to 10 (LER) and 4 (HER) stations. In addition, countermeasures against RF-related instabilities in LLRF are essential for the high beam current operation. These measures have been completed partially. Remaining update items will be performed in the future to achieve the target beam current and luminosity. The details of upgrade of each component are described in Refs. [9, 13–18]. In this report, the operation status of RF system and the high beam current-related issues in RF system are described.

OPERATION STATUS OF RF SYSTEM

In the recent beam operation, the RF system is operating stably without any troubles requiring long shutdown.

* michiru.nishiwaki@kek.jp

ISBN: 978-3-95450-236-3 ISSN: 2673-7027 doi:10.18429/JACoW-eeFACT2022-WEXAS0102

Table 1: RF-related machine parameters achieved at KEKB [12] and those of the design values in SuperKEKB [6].

		KEKB (achieved)				SuperKEKB (design)			
Parameters	**Unit**	**LER**	**HER**			**LER**		**HER**	
Beam energy	GeV	3.5	8.0			4.0		7.0	
Beam current	A	2.0	1.4			3.6		2.6	
Bunch length	mm	6–7	6–7			6		5	
Number of bunch		1585	1585			2500		2500	
Total RF voltage	MV	8	13–15			10–11		15	
Energy loss/turn	MV	1.6	3.5			1.76		2.43	
Total beam power	MW	3.3	5.0			~8		~8	
RF frequency	MHz	508.9				508.9			
Revolution frequency	kHz	99.4				99.4			
Cavity type		ARES	ARES		SCC	ARES		ARES	SCC
No. of cavities		20	10	2	8	8	14	8	8
Klystron : cavities		1:2	1:2	1:1	1:1	1:2	1:1	1:1	1:1
No. of klystron stations		10	5	2	8	4	14	8	8
RF voltage/cavity	MV	0.4	0.31	0.31	1.24	~0.5	~0.5	~0.5	1.3–1.5
Beam poser/cavity	kW	200	200	550	400	200	600	600	400
R/Q of cavity	Ω	15	15	15	93	15	15	15	93
Loaded Q (Q_L)	$\times 10^4$	3	3	1.7	~5	3	1.7	1.7	~5

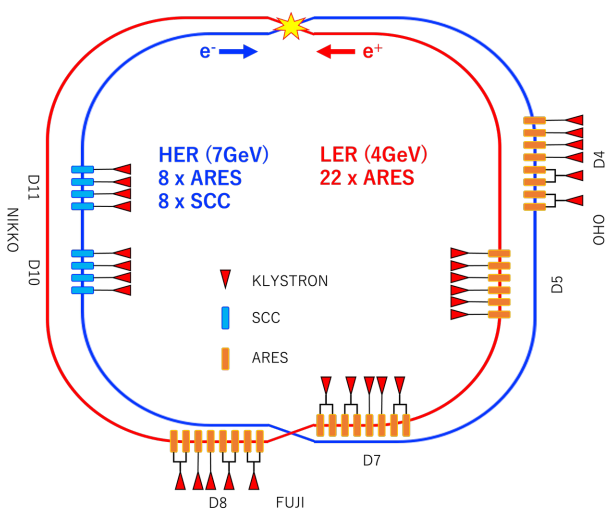

Figure 1: Layout of RF system of SuperKEKB. There are a total of 30 RF stations consisting both of normal-conducting cavity (ARES) and superconducting cavity (SCC) stations.

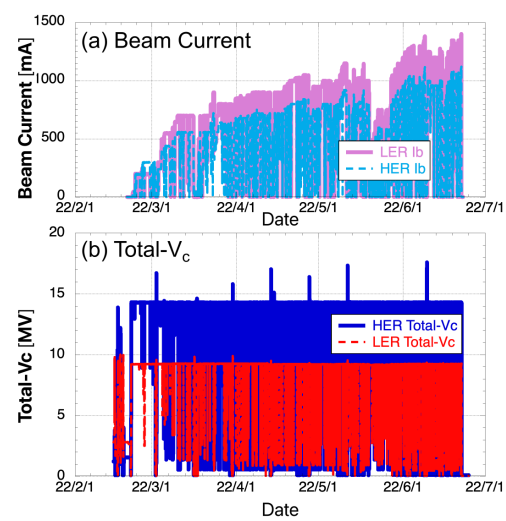

Figure 2: Operation history of 2022ab run. (a) shows beam current of LER (pink) and HER (cyan). (b) indicates total-V_c of LER (red) and HER (blue). The spikes in total-V_c are correspond to cavity aging in regular maintenance day.

Figure 2 shows the history of the beam current and total-V_c for both rings in the run of 2022ab (from Feb. to June 2022). In this run, the beam current was gradually increased while increasing the number of bunches, finally achieved up to 1.46 A for LER and 1.14 A for HER with 2346 bunches. The total-V_c for both rings were kept as 9.12 MV for LER and 14.2 MV for HER through this run. After middle of April, although one of ARES 1:1 stations (D07C) in LER was detuned (parked) due to a problem with the control system of the klystron power supply, the total-V_c was able to be maintained by increasing the voltage of other cavities. The voltage of each ARES cavity was 0.40–0.45 MV/cavity. In SCC, the cavity voltage was 1.35 MV/cavity. The spikes of total-V_c shown in Fig. 2(b) are correspond to cavity aging in regular maintenance days. The drop downs of total-V_c are the results of beam aborts. When the beam higher than 300 mA is aborted (dumped instantaneously), the RF is turned off by the interlock of the reflection power from the cavity in almost all RF stations. Conversely, if the interlock works even at one RF station and the RF is turned off, the beam of the corresponding ring is aborted.

Figure 3 shows the power delivered to beam by each cavity as a function of the stored beam current. For the maximum

ISBN: 978-3-95450-236-3 ISSN: 2673-7027 doi:10.18429/JACoW-eeFACT2022-WEXAS0102

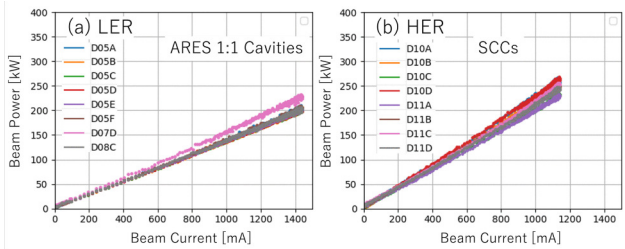

Figure 3: Beam power of each cavity as a function of the stored beam current. (a) shows ARES 1:1 cavities in LER. (b) shows SCCs in HER. The beam power is obtained by subtracting the reflected power from the cavity and the cavity wall loss from the klystron output or cavity input power.

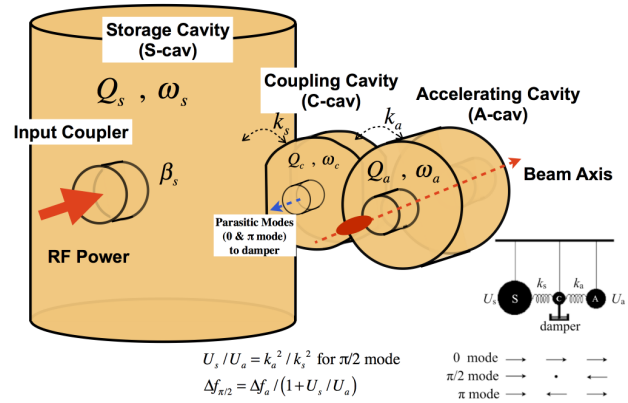

Figure 4: Illustration of the ARES cavity structure.

beam current, the beam power was reached to ~230 kW in an 1:1 ARES cavity in LER (Fig. 3(a)) and ~260 kW in a SCC in HER (Fig. 3(b)). In higher beam current operation, the optimization of the beam loading balance among the RF stations will be essential for stable and efficient beam operation. The optimization tool has been established and used in the actual beam operation [19].

All beam aborts are analyzed by recording the RF and beam signals to find the cause of trip. In particular, in ARES stations with digital LLRF system, all RF signals are recorded with a resolution of around 0.1 µs in maximum before and after events such as abort and RF off [16]. The fast-signal monitor is very useful as a diagnosis tool for the RF system. The number of beam aborts caused by the RF system was ~10% of all aborts (725 aborts in 2022ab), excluding manual and low current (<50 mA) aborts. The ~35% of the RF aborts were due to breakdown of ARES cavities and SCCs. In the 2022ab operation, the trip rates due to breakdown were ~0.5/cavity for the 30 ARES cavities and ~0.9/cavity for the 8 SCCs in four months operation. The trip rates of cavities are not changed significantly since KEKB operation. The ~40% of the RF aborts were due to HPRF system including incorrect operation of the interlock system of the klystron power supply system. As mentioned above, in 2022ab run, one klystron station was disconnected from the beam operation because the heater power supply of the klystron was broken due to a control board failure. One of the causes of problems on the HPRF system is the deterioration of the devices and infrastructure due to aging. Also in LLRF system, the aging of analog control modules is main cause of the failures. For stable operation, regular inspections and updating of devices are being carried out throughout the RF system.

ARES CAVITY

The ARES is a unique cavity, which is specialized for KEKB [7, 8]. It consists of a three-cavity system operated in the $\pi/2$ mode: the accelerating (A-) cavity is coupled to a storage (S-) cavity via a coupling (C-) cavity as shown in Figure 4 [9]. The A-cavity is structured to damp HOM. The S-cavity with a large stored energy plays a role in suppressing the optimum detuning of accelerating $\pi/2$ mode ($f_{\pi/2}$). Corresponding to the stored energy ratio of $U_s/U_a = 9$, where U_s and U_a are stored energies of S- and A-cavities, the detuning of $\pi/2$ mode ($\Delta f_{\pi/2}$) is one tenth that of A-cavity (Δf_a). As a result, the coupled bunch instabilities driven by the accelerating mode is suppressed. The C-cavity is equipped with a damper to damp parasitic 0 and π-modes. The $\pi/2$ mode has a high Q value of ~110,000 and a low R/Q value of 15 Ω.

The high-power input coupler has been upgraded to cope with the large beam power of SuperKEKB. At the design beam current, the beam power of 1:1 ARES is estimated as 600 kW in a cavity and the input power become to be 800 kW including the cavity wall loss of around 150 kW. In order to increase the input power from 400 to 800 kW, the coupling factor β of the input coupler has been increased from 3 to 5 [6, 14]. In addition, to suppress multipactoring problem in the coaxial lines of the couplers, the fine groove structure is adopted for the outer conductor surface (Fig. 5) [13]. 14 of the 32 input couplers have been upgraded with an increased coupling factor β of 5 and the fine groove structure. Those new input couplers have no multipactoring and other problems in SuperKEKB beam operation so far.

At higher beam current operation, diagnostic tools will become more important. In the ARES system, all input couplers are monitored with TV or network cameras attached to the viewport of S-cavity on the opposite side of the input coupler. A few seconds of video of the camera before and after the RF is turned off is automatically recorded on mass storage devices. Figure 6 shows examples of the recorded videos with the cameras. This diagnostic tool can isolate the problem; it is related to the input coupler or not. Another diagnostic tool is fast-signal recording by the digital LLRF. Figure 7 shows examples of the fast signals with a microsecond resolution. When the RF switch is turned off due to a reason other than the cavity, the field falls with a tail determined from the fill time (~10 µs) as seen in Fig. 7(a). On the other hand, as seen in Fig. 7(b), the field drops in a much shorter time than the fill time, which can be understood as an occurrence of cavity breakdown due to vacuum arc.

ISBN: 978-3-95450-236-3 ISSN: 2673-7027 doi:10.18429/JACoW-eeFACT2022-WEXAS0102

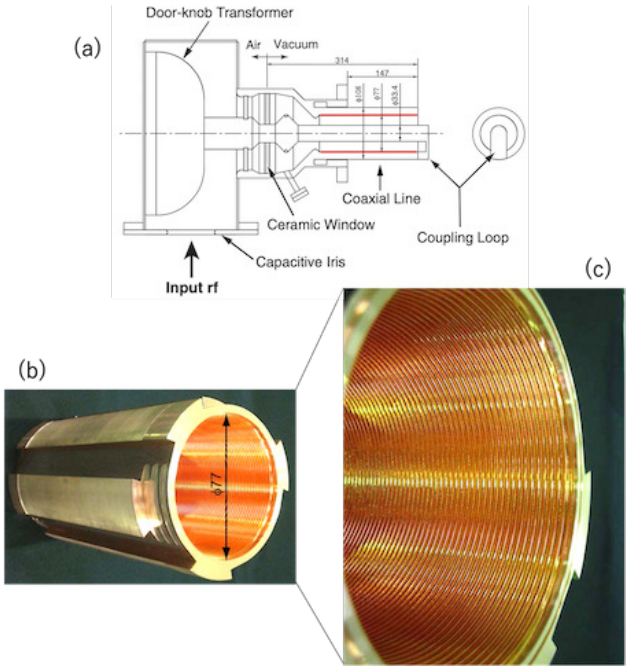

Figure 5: Schematic view of input coupler for the ARES(a), outer conductor with fine grooving (b) and zoom of fine grooving(c). The red line in (a) indicate the fine grooving structure.

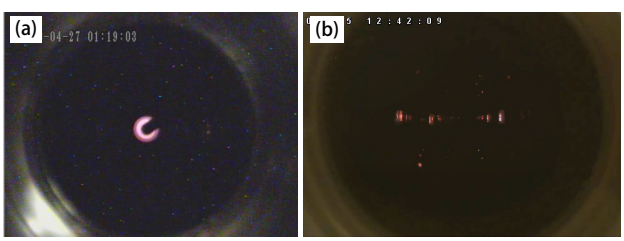

Figure 6: Examples of the recorded videos with the cameras attached to the viewport of S-cavity on the side opposite the input coupler at the moment of cavity trips. (a) Clear discharge from multipactoring on the RF window in the input coupler was observed. (b) Lights came not from the input coupler but some other place with scattered reflection.

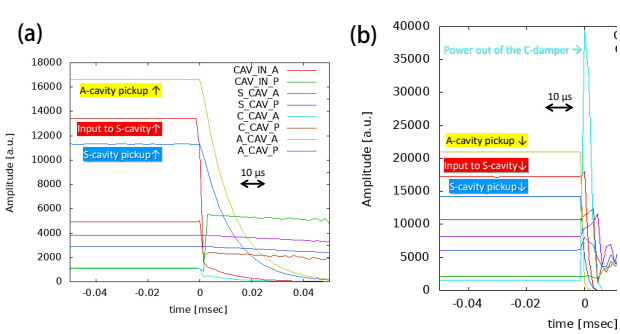

Figure 7: Examples of the fast signals recorded by the digital LLRF; (a) when the RF switch was turned off manually, (b) cavity breakdown event.

SCC MODULE

The SCC modules (Fig. 8) [10] and cryogenic system [20] are also reused from KEKB. The SCC module was designed for KEKB with HOM damped structure equipped with a pair of ferrite HOM dampers on both small beam pipe (SBP) and large beam pipe (LBP) [21]. The beam power and accelerating voltage are kept by sharing with ARES cavities by giving phase-offset.

The handling large HOM powers induced by the high beam current is one of the main issues. According to the power flow simulation in one cavity module, the load of the existing a pair of ferrite dampers is around 20 kW, which is not much increased from the maximum absorbed power of 16 kW in KEKB operation [11]. But large HOM power is emitted through the downstream beam duct and the power becomes additional load of the dampers of downstream cavity [22]. To reduce the emission power, two sets of additional HOM dampers made by SiC have been installed to the downstream of two SCC modules [17, 23]. In the beam operation, the HOM power absorbed by the ferrite dampers of downstream cavities were reduced by more than 10% by the additional SiC dampers as shown in Fig. 9. The absorbed HOM power by a pair of ferrite dampers in one SCC module were ~8 kW at the maximum beam current in 2022ab. To achieve design beam current, SiC dampers will be installed to downstream of all cavities.

Another issue is degradation of the cavity performance of Q_0. In the long-term operation since 1998, SCCs experienced several vacuum works and troubles. As a result, performance of several cavities degraded with strong field emission. To recover the cavity performance, we developed horizontal high-pressure rinse (HHPR) method [24]. By HHPR, the performance of three cavities have been success-

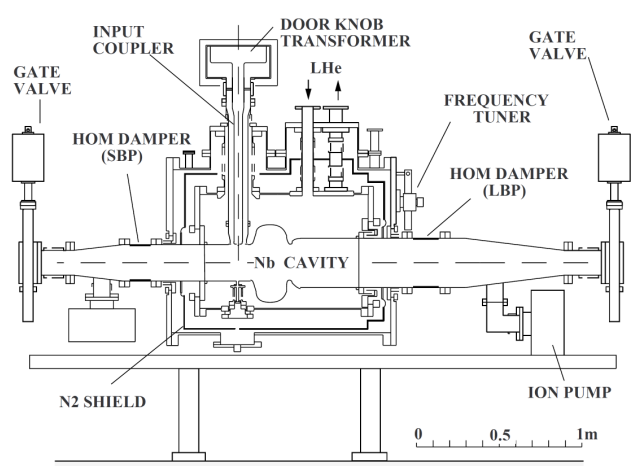

Figure 8: Cross-sectional view of HOM damped SCC designed for KEKB. This cavity is used for SuperKEKB. Ferrite HOM dampers are equipped on both SBP and LBP. The SBP and LBP diameters are 220 mm and 300 mm, respectively.

ISBN: 978-3-95450-236-3 ISSN: 2673-7027 doi:10.18429/JACoW-eeFACT2022-WEXAS0102

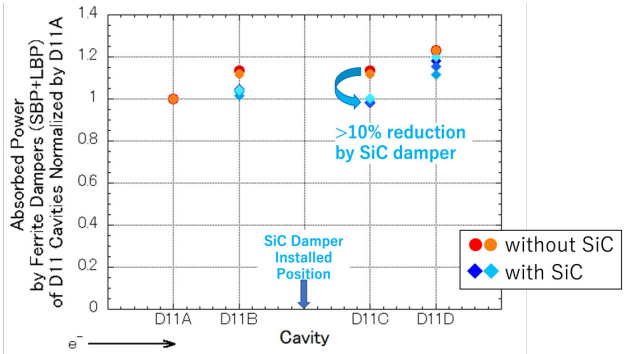

Figure 9: Ratio of absorbed HOM power by ferrite dampers of SCC cavities in D11 section.

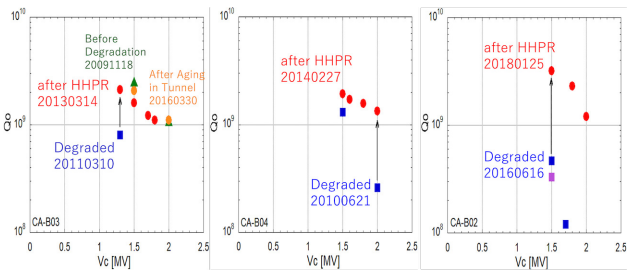

Figure 10: Q_0 values as a function of V_c before and after HHPR for three degraded cavities.

fully recovered as shown in Fig. 10 and those cavities are operating stably in SuperKEKB.

In the beam operation, the RF signals are monitored by oscilloscopes every beam aborts to analyze the cause of trip. Figure 11 shows an example of a trip by multipacting in cavity. The spike of V_c (cavity pickup) signal was found ~40 ms before RF turned off by the interlock from the breakdown detector (Fig. 11(a)). It is supposed that the multipacting occurred and disappeared in a few tens of microseconds (Fig. 11(b)), and the local normal conducting region generated by the multipacting gradually propagated, increasing the cavity wall loss. Finally, an increase in klystron output power was observed as a result of feedback control to keep V_c constant (Fig. 11(c)). It is important to detect malfunctions of SRF system quickly by the diagnostic system in order to continue stable operation at high beam currents.

HIGH BEAM CURRENT-RELATED ISSUES IN RF SYSTEM

The RF issues to be considered for the high beam current are summarized in Ref. [25]. In SuperKEKB, coupled bunch instability (CBI) excited by accelerating mode and an effect of bunch gap transient is estimated to be problem in high beam current operation. The countermeasures in SuperKEKB are introduced below. For CBI due to HOM, the ARES and SCC are designed as HOM dumped structures and equipped with HOM dampers [7, 10]. Additionally the bunch-by-bunch feedback system is effective for damping the instability.

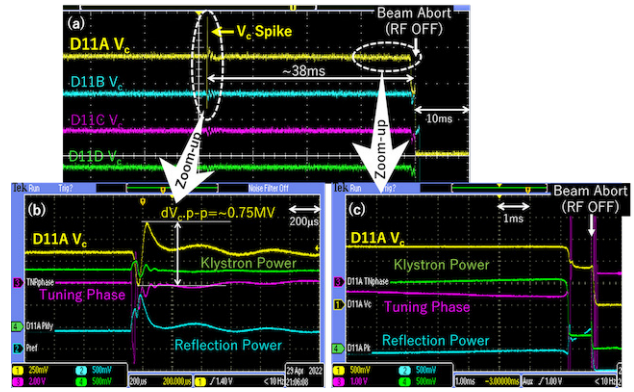

Figure 11: Example of RF signals of a trip event of D11A cavity monitored by oscilloscopes; (a) long-range monitor of V_c of 4 cavities, (b) focused on V_c spike event, (c) focused on just before beam abort. The V_c (yellow), klystron output power (green), cavity reflection power (cyan) and cavity tuning phase (magenta) are indicated in (b) and (c).

CBI due to $\mu = -1, -2$ and -3 Mode [18, 26]

The growth rates of CBI due to accelerating mode are estimated as shown in Figure 12 for SuperKEKB LER (upper) and HER (lower side) [18]. The threshold of beam currents for $\mu = -1$ mode are less than the design currents in both of LER and HER. The dashed lines show the damping rates with a parked (detuned) cavity. In that case, the thresholds of $\mu = -2$ mode are also below the design currents for both ring. In HER operation, CBI of $\mu = -1$ mode is excited at lower beam current than expected, but the cause is still not clear. Though it is necessary to investigate the cause, CBI damper is essential in order to continuing beam operation.

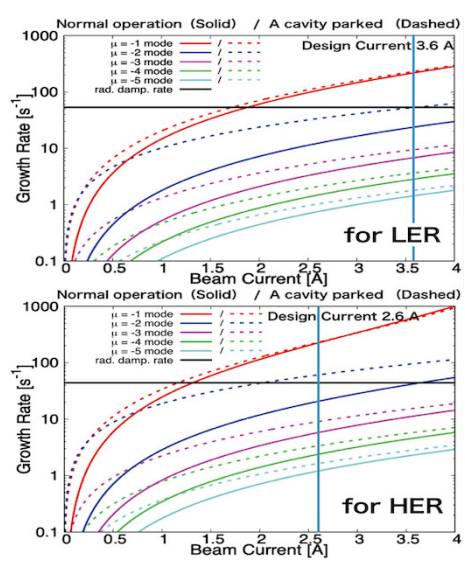

Figure 12: Estimation of the growth rate of the coupled bunch instability due to accelerating mode of $\mu = -1, -2$ and -3. Upper and lower side indicate for LER and HER, respectively.

ISBN: 978-3-95450-236-3 ISSN: 2673-7027 doi:10.18429/JACoW-eeFACT2022-WEXAS0102

In LLRF system of SuperKEKB, new damper system with new digital filters for CBI has been developed [18]. The damper system is installed to ARES station with digital LLRF system. The damper system can correspond to $\mu = -1, -2$ and -3 modes in parallel as shown in Fig. 13 [26]. Figure 14 shows examples of beam spectra without (upper side) and with (lower side) CBI damper [18]. In that case, $\mu = -2$ mode was excited intentionally by detuning one SCC of −200 kHz in HER. One can see a peak in upper spectra at frequency of $f_{rf} - 2f_0 + f_s$, where f_{rf} is RF frequency of 508.876 MHz, f_0 is revolution frequency of 99.4 kHz and f_s is synchrotron frequency of 2.78 kHz in design [6]. After tuning of phase and amplitude of the CBI damper, the peak is disappeared in lower spectra. The new CBI damper has been operating from Phase-2 operation (2019) in both rings. The CBI is not a problem with this damper systems up to 1.46 A for LER and 1.14 A for HER.

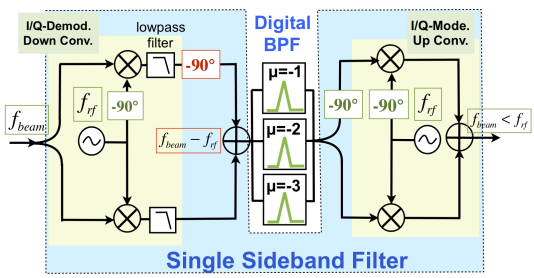

Figure 13: Block diagram of new digital filter with single sideband filter for CBI damper. The digital filter is available for the $\mu = -1, -2$ and -3 modes in parallel.

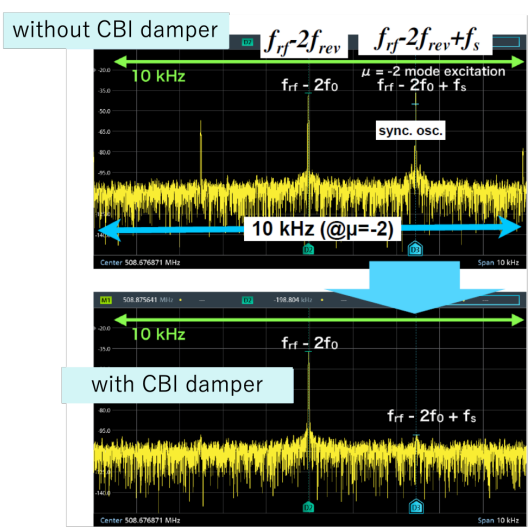

Figure 14: Example of beam spectra without (up) and with (bottom) CBI damper for $\mu = -2$ mode.

Stability of the Zero Mode under heavy beam loading [27, 28]

In SuperKEKB high-current beam operation, achieving the stability of the zero mode associated with the accelerating mode of the RF system is an important concern because of heavy beam loading. The stability criterion can be more severe compared to the Robinson's one [29] by the effects of control functions in the LLRF system including amplitude and phase control loops for the cavity field. The issue is a more serious problem in the HER compared to the LER because of high impedance of superconducting cavities operating in the HER.

As a countermeasure, the RF system is equipped with a direct RF feedback system (DRFB) to effectively reduce the impedance of the cavities and a zero mode oscillation damper (ZMD). Although the DRFB and ZMD were also used at KEKB to mitigate the beam loading [30], they have more significant roles in SuperKEKB because of higher beam current. Figure 15 shows a schematic view of the LLRF system, highlighting an SCC station (D11-A). Because the bandwidths of the amplitude and phase control loops are much less than the revolution frequency, 99.4 kHz, these loops do not interact with the beam at the higher coupled modes such as −1, −2, −3 modes, but are intertwined with the beam, DRFB, and ZMD in the zero mode.

The stability of the zero mode for the system was quantitatively analyzed with heavy beam loading, taking these loops into account [28]. Two different approaches were used in the analysis: One was based on the characteristic equation (CE) and the other using a simulation in the time domain. First, the consistency between both methods was confirmed by applying them to typical cases. Next, the simulation results were compared to measurements performed in a machine study conducted in 2019 [27] during SuperKEKB beam operation. Figure 16 shows the zero-mode coherent synchrotron frequency f_s as a function of the beam current at different DRFB gains obtained from the simulation (blue and black marks), as well as the measured values in the machine study (red marks). In both the simulation and measurement, f_s

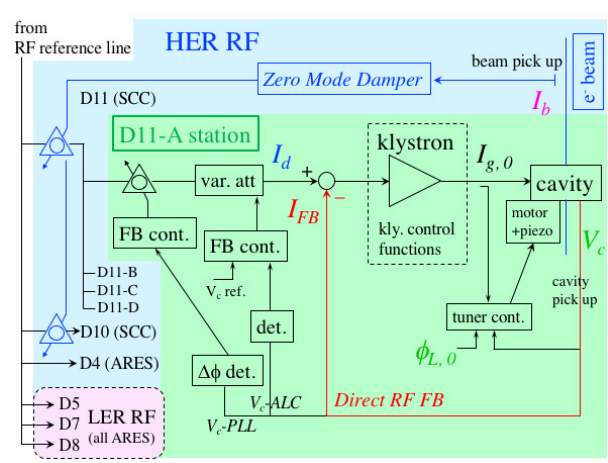

Figure 15: Schematic view of LLRF system for SuperKEKB, highlighting an SCC station (D11-A) in green colored part. In addition to the amplitude and phase control loops for the cavity field, the DRFB and ZMD are implemented. Cavity tuning is performed based on the relative phase between the klystron output and cavity voltage.

ISBN: 978-3-95450-236-3 ISSN: 2673-7027 doi:10.18429/JACoW-eeFACT2022-WEXAS0102

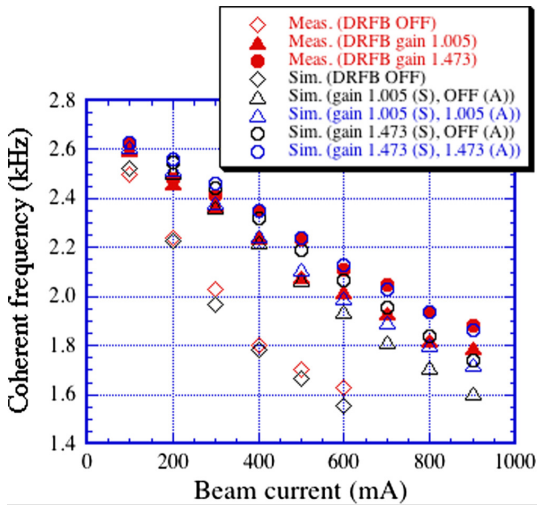

Figure 16: Calculated and measured frequencies of the zero-mode coherent synchrotron oscillation f_s with SCC and ARES in the HER as a function of the stored beam current. The blue (black) marks correspond to the DRFB for ARES on (off) in the simulation. The red marks show measured values in the beam study [27]. The circle (triangle) marks indicate the DRFB gain of 1.473 (1.005). The diamond marks indicate DRFB off (from [28]).

decreased as the beam current increased owing to beam loading and the effect of the DRFB on reducing the f_s shift was clearly observed. The simulation and measurement results were in good agreement.

Having confirmed the validity of these methods, analysis using the CE and simulation were comprehensively conducted for future high-current beam operations in SuperKEKB. The results showed the effectiveness of DRFB and ZMD, which played an important role in ensuring the zero mode stability. In beam operations, maximum achievable stored current may be considerably lower than the threshold current obtained from the analysis for different reasons such as: scattering the cavity performance or operating conditions, nonlinearities of klystrons and other RF components, and fluctuations caused by unknown jitters and machine errors. Because it is difficult to quantitatively predict these uncertain effects, we searched parameter sets that provided sufficient high threshold currents compared to the design currents. Here, as reference guideline, a threshold current target value of 4 A (5 A) in the HER (LER) was set because it was considered to be a good margin for the design current of 2.6 A (3.6 A), although it had not yet been validated for the operation. Efforts to obtain more reliable confirmation on this would be continued in the beam operation with increasing beam current step by step. Thus, different operational parameter sets as well as possible system modifications were investigated, thereby creating a considerably good margin to compensate for the possible deficiencies at higher beam currents. The results could be used as guidelines for future beam operation by increasing the beam current step by step. For more details, see Ref. [28].

Bunch Gap Transient [31, 32]

In a multi-bunch storage ring, bunch trains have an empty-bucket gap to ensure the rise time of the beam abort kicker. However, the gap modulates the amplitude and phase of an accelerating cavity field. As a result, the longitudinal synchronous position is shifted bunch by bunch along the train. For colliders such as SuperKEKB, the collision point shift is causing a loss of luminosity. Figure 17 shows an example of RF phase modulation of the accelerating cavity of ARES (D05A) measured with digital LLRF system in the beam current of 1 A in LER. The blue solid line is measured and red dashed line is simulated results. The horizontal axis is time in microseconds. The time interval of 10 μs is the revolution period. In recent operation, we have two abort gaps in one revolution to be short the wait time for abort. The rapid phase change was observed at the leading part of train. From the results of new simulation studies for the bunch gap transient [31], the rapid phase change at the leading part is caused by a transient loading in the three-cavity system of ARES (Fig. 4). In other words, the rapid phase change is due to the parasitic (0 and π) modes of ARES.

The collision point shift can be estimated from a phase difference between LER and HER. Figure 18 shows the phase difference between LER and HER ($\Delta\phi_{HER} - \Delta\phi_{LER}$) of the gap region, obtained from the simulation with the SuperKEKB design parameters (the gap length of 2%). The red solid line indicates the relative phase. As one can see, the maximum phase difference will be 5.5° (pk-pk) at the leading part of collision bunches. The phase shift of 5.5° corresponds to a longitudinal displacement of $0.44\sigma_z$ at the collision point, where the bunch length (σ_z) is 5 mm (rms). Except the leading part, the phase difference along the train is not so large (< 1°).

Because, in SuperKEKB, the crossing angle between the two beams at the collision point is larger and the vertical beta

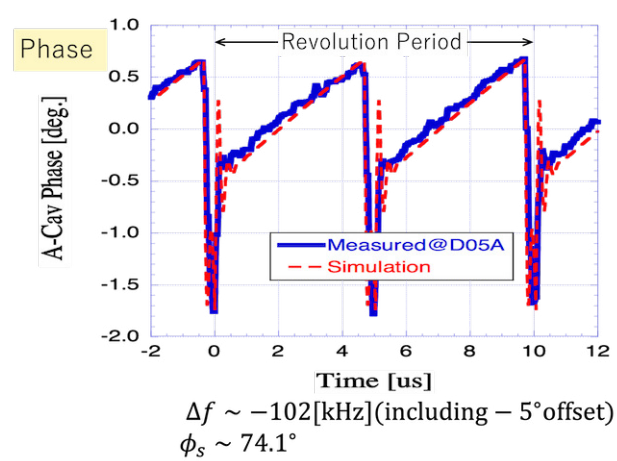

Figure 17: RF phase modulation in the accelerating (A-) cavity of ARES in LER. Blue solid line is measured and red dashed line is simulated results. The beam current was around 1 A. There are two abort gaps i.e. two trains in the revolution period of 10 μs.

ISBN: 978-3-95450-236-3 ISSN: 2673-7027 doi:10.18429/JACoW-eeFACT2022-WEXAS0102

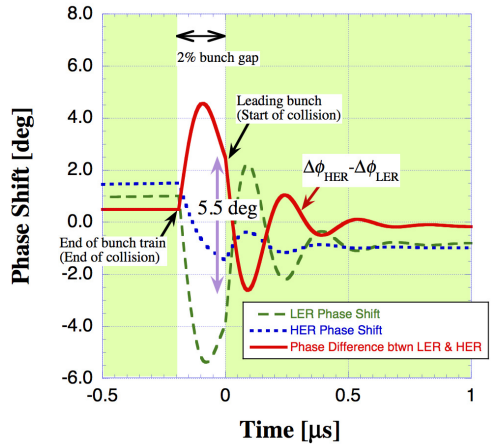

Figure 18: Phase difference between LER and HER (red solid line = $\Delta\phi_{HER} - \Delta\phi_{LER}$). Zoomed the gap region.

function is much smaller than those of KEKB, the effect of the large phase difference might be crucial issue to achieve high luminosity. Unfortunately, the feed-forward control cannot be available in our RF system to mitigate the phase modulation due to the gap transient, because the klystron performance (the bandwidth of ~100 kHz and the output power) is not enough to cancel the rapid phase modulation.

We have proposed the method to mitigate the phase difference [31]. The first point of the mitigation method is making a delay of the HER gap timing with respect to the LER gap. The second point is to increase the bunch current in the leading part of LER in a step-like manner as shown in Fig. 19. The HER gap is delayed by d_g. The bunch current in the leading part of LER is increased in two steps with a time interval w_s with the step height of b_s. g_L and g_H are the gap lengths of LER and HER, respectively, and are set to 2% ($g_L = g_H = 200$ ns), which is the minimum length required from the rise time of the abort kicker. b_s is set to half of the nominal bunch current for simplicity. The simulation was performed by changing the parameters d_g and w_s. The best result was obtained with $d_g = 160$ ns and $w_s = 140$ ns. The result is shown in Fig. 20. The phase difference between LER and HER is reduced to 0.4° at the leading part of the collision as shown in Fig. 20(b), while the phase difference along the train is kept small as shown in Fig. 20(a). From the simulation, it is found that the fill pattern change of LER in addition to the HER delay gives more effective mitigation. For more details, see Ref. [31]. In actual operation, it is necessary to optimize the fill pattern and gap delay while observing the luminosity.

SUMMARY

SuperKEKB is steadily increasing the beam current and continues to update own luminosity record. The RF system of SuperKEKB is operating stably at large beam current of 1.14 A for HER and 1.46 A for LER in 2022ab operation. The cavities are operating stably with low trip rates. The ARES and SCC systems have been upgraded to handle the

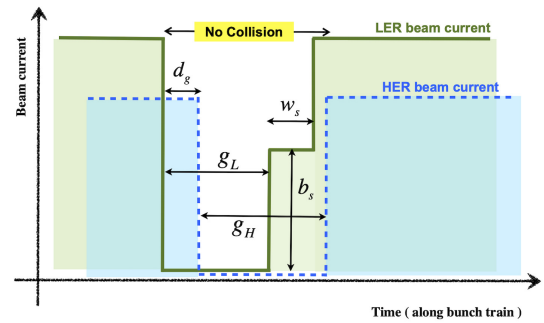

Figure 19: Illustration of a bunch fill pattern for more effective mitigation. HER gap is delayed by d_g. The bunch current in the leading part of LER is increased in two steps with a time interval w_s with the step height of b_s. g_L and g_H are the gap length of LER and HER, respectively.

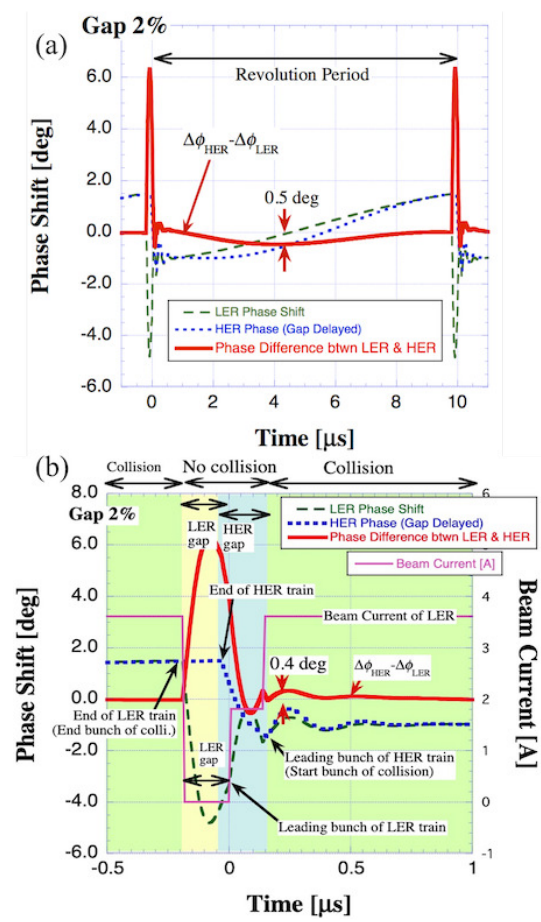

Figure 20: Phase difference between LER and HER with the mitigation method of Fig. 19. The HER delay $d_g = 160$ ns and the LER step height $w_s = 140$ ns. Bottom plot (b) is zoom of the gap region of upside plot (a).

ISBN: 978-3-95450-236-3 ISSN: 2673-7027 doi:10.18429/JACoW-eeFACT2022-WEXAS0102

high beam current and the large beam power. For ARES, the input coupler has been upgraded with increasing coupling factor and the fine grooving structure. The couplers have no problems in the beam operation. It is confirmed that the additional SiC HOM dampers for SCC reduce HOM load of ferrite dampers of downstream cavities. In the future, SiC dampers will be installed to downstream of all cavities. To control instabilities, such as CBI and coherent oscillation due to large beam current, CBI damper, DRFB and ZMD are established and working well. Comprehensive analysis using the CE and simulations showed the effectiveness of DRFB and ZMD in ensuring zero-mode stability, as well as guidelines for future beam operations by increasing the beam current step by step. The mitigation method of the beam phase difference between LER and HER due to the bunch gap transient effect is proposed: the relative phase change at IP can be reduced by optimization of the gap delay and bunch fill pattern.

REFERENCES

[1] Y. Ohnishi *et al.*, "Accelerator Design at SuperKEKB", Prog. Theor. Exp. Phys., vol. 2013, no. 3, p. 03A011, 2013. https://doi.org/10.1093/ptep/pts083

[2] Y. Funakoshi *et al.*, "The SuperKEKB Has Broken the World Record of the Luminosity", in *Proc. IPAC'22*, Bangkok, Thailand, Jun. 2022, pp. 1–5. doi:10.18429/JACoW-IPAC2022-MOPLXGD1

[3] Y. Ohnishi, "SuperKEKB Luminosity Quest", presented at the 65th ICFA Advanced Beam Dynamics Workshop on High Luminosity Circular e+e- Colliders (eeFACT22), Frascati (RM), Italy, Sept. 2022, this workshop.

[4] K. Akai *et al.*, "RF Systems for the KEK B-Factory", Nucl. Instrum. Methods Phys. Res., Sect. A499, 45 (2003). https://doi.org/10.1016/S0168-9002(02)01773-4

[5] K. Akai *et al.*, "RF System for SuperKEKB", in *Proc. of the 7th Annual Meeting of Particle Accelerator Society of Japan*, Himeji, Japan, Aug. 4-6, 2010, pp. 177–181. https://www.pasj.jp/web_publish/pasj7/proceedings/SH_4PM_2/WESH05.pdf

[6] SuperKEKB Design Report, RF System, 2014. https://www-linac.kek.jp/linac-com/report/skb-tdr/6_RF_190131b_pp149-215Akai.pdf

[7] Y. Yamazaki and T. Kageyama, "A Three-Cavity System which Suppresses the Coupled-Bunch Instability Associated with the Accelerating Mode", Part. Accel., 44, 107 (1993).

[8] T. Kageyama *et al.*, "The ARES Cavity for KEKB", in *Proc. APAC'98*, Tsukuba, Japan, Mar. 1998, pp. 773-775 (1998). https://accelconf.web.cern.ch/a98/APAC98/6D039.PDF

[9] T. Kageyama, T. Abe, H. Sakai, Y. Takeuchi and K. Yoshino, "ARES Cavity System for SuperKEKB", in *Proc. of the 8th Annual Meeting of Particle Accelerator Society of Japan*, Tsukuba, Japan, Aug. 1-3, 2011, pp. 1245–1249. https://www.pasj.jp/web_publish/pasj8/proceedings/poster/TUPS126.pdf

[10] T. Furuya *et al.*, "Recent Status of the Superconducting Cavities for KEKB", in *Proc. SRF'99*, Santa Fe, NM, USA, Nov. 1999, paper MOP001, pp. 31–36. https://accelconf.web.cern.ch/SRF99/papers/mop001.pdf

[11] Y. Morita *et al.*, "Status of KEKB Superconducting Cavities and Study for Future SKEKB", in *Proc. SRF'09*, Berlin, Germany, Sep. 2009, paper TUPPO022, pp. 236–238. https://accelconf.web.cern.ch/SRF2009/papers/tuppo022.pdf

[12] T. Abe *et al.*, "Performance and Operation Results of the RF Systems at the KEK B-Factory", Prog. Theor. Exp. Phys. 2013, 03A006 (2013). https://doi.org/10.1093/ptep/ptt020

[13] T. Abe, T. Kageyama, H. Sakai, Y. Takeuchi and K. Yoshino "Multipactoring Suppression by Fine Grooving of Conductor Surfaces of Coaxial-line Input Couplers for High Beam Current Storage Rings", Phys. Rev. Accel. Beams 13, 102001 (2010). https://link.aps.org/doi/10.1103/PhysRevSTAB.13.102001

[14] T. Kageyama, K. Yoshino, H. Sakai, T. Abe and Y. Takeuchi, "Input Coupler for the ARES Cavity in SuperKEKB", in *Proc. of the 11th Annual Meeting of Particle Accelerator Society of Japan*, Aomori, Japan, Aug. 9-11, 2014, pp. 590–594. https://www.pasj.jp/web_publish/pasj2014/proceedings/PDF/SAP0/SAP044.pdf

[15] K. Watanabe, M. Yoshida, S. Yoshimoto, K. Marutsuka and M. Ono, "Current Status of the High-Power RF Systems in MR for Super-KEKB", in *Proc. of the 12th Annual Meeting of Particle Accelerator Society of Japan*, Tsuruga, Japan, Aug. 5-7, 2015, pp. 630–633. https://www.pasj.jp/web_publish/pasj2015/proceedings/PDF/WEP0/WEP065.pdf

[16] T. Kobayashi *et al.*, "Development and Construction Status of New LLRF Control System for SuperKEKB", in *Proc. IPAC'14*, Dresden, Germany, Jun. 2014, pp. 2444–2446. doi:10.18429/JACoW-IPAC2014-WEPME071

[17] M. Nishiwaki, K. Akai, T. Furuya, A. Kabe, S. Mitsunobu and Y. Morita, "Operation Status of Superconducting Accelerating Cavity and Development of SiC Damper for SuperKEKB", in *Proc. of the 14th Annual Meeting of Particle Accelerator Society of Japan*, Sapporo, Japan, Aug. 1-3, 2017, pp. 914-918. https://www.pasj.jp/web_publish/pasj2017/proceedings/PDF/WEP0/WEP037.pdf

[18] K. Hirosawa, K. Akai, E. Ezura, T. Kobayashi, K. Nakanishi and S. Yoshimoto, "Advanced Damper System with a Flexible and Fine-tunable Filter for Longitudinal Coupled-bunch Instabilities Caused by the Accelerating Mode in SuperKEKB", Nuclear Inst. and Methods in Physics Research, A 953 (2020) 163007. https://doi.org/10.1016/j.nima.2019.163007

[19] S. Ogasawara, K. Akai, T. Kobayashi, K. Nakanishi and M. Nishiwaki, "Optimization of RF Phase and Beam Loading Distribution among RF Stations in SuperKEKB", presented at the The Low Level RF Workshop 2022 (LLRF22), Brugg-Windisch, Switzerland, Sept. 2022.

[20] K. Nakanishi *et al.*, "KEKB/SuperKEKB Cryogenics Operation", in *Proc. eeFACT'18*, Hong Kong, China, Sep. 2018, pp. 276. doi:10.18429/JACoW-eeFACT2018-WEPAB04

[21] T. Tajima, "Development of Higher-Order-Mode (HOM) Absorbers for KEKB Superconducting Cavities", KEK

ISBN: 978-3-95450-236-3 ISSN: 2673-7027 doi:10.18429/JACoW-eeFACT2022-WEXAS0102

Report 2000-10 (2000). https://lib-extopc.kek.jp/preprints/PDF/2000/0024/0024010.pdf

[22] M. Nishiwaki, K. Akai, T. Furuya, A. Kabe, S. Mitsunobu and Y. Morita, "Developments of SiC Damper for SuperKEKB Superconducting Cavity", in *Proc. SRF'15*, Whistler, Canada, Sep. 2015, paper THPB071, pp. 1289–1292. http://srf2015.vrws.de/papers/thpb071.pdf

[23] M. Nishiwaki, K. Akai, T. Furuya,S. Mitsunobu and Y. Morita, "Status of Superconducting Accelerating Cavity at SuperKEKB Phase-2 Operation", in *Proc. of the 15th Annual Meeting of Particle Accelerator Society of Japan*, Nagaoka, Japan, Aug. 7-10, 2018, pp. 428-432. https://www.pasj.jp/web_publish/pasj2018/proceedings/PDF/WEP0/WEP049.pdf

[24] Y. Morita, K. Akai, T. Furuya, A. Kabe, S. Mitsunobu and M. Nishiwaki, "Developments of Horizontal High Pressure Rinsing for SuperKEKB SRF Cavities", in *Proc. SRF'15*, Whistler, Canada, Sep. 2015, paper MOPB116, pp. 443–447. https://jacow.org/SRF2015/papers/MOPB116.pdf

[25] K. Akai, "RF Issues for High Intensity Factories", in *Proc. EPAC'96*, Sitges, Spain, Jun. 1996, paper TUX03A, pp. 205-209 (1996). https://accelconf.web.cern.ch/e96/PAPERS/ORALS/TUX03A.PDF

[26] T. Kobayashi, "RF system (2)", OHO'19 (2019).

[27] K. Akai, A. Kabe, T. Kobayashi, K. Nakanishi and M. Nishiwaki, "Verification of RF Feedback to Suppress Longitudinal Instability due to Beam Loading in SuperKEKB", in *Proc. of the 10th Annual Meeting of Particle Accelerator Society of Japan, 2020*, p.320. https://www.pasj.jp/web_publish/pasj2020/proceedings/PDF/WEPP/WEPP35.pdf

[28] K. Akai, "Stability Analysis of RF Accelerating Mode with Feedback Loops under Heavy Beam Loading in SuperKEKB", Phys. Rev. Accel. Beams 25, 102002 (2022). https://doi.org/10.1103/PhysRevAccelBeams.25.102002

[29] K. W. Robinson, "Stability of beam in radiofrequency system, Cambridge Electron Accelerator", Report No. CEAL-1010 (1964).

[30] K. Akai, N. Akasaka, K. Ebihara, E. Ezura, M. Suetake and S. Yoshimoto, "The Low-Level RF System for KEKB", in *Proc. EPAC'98*, Stockholm, Sweden, Jun. 1998, paper TUP10G, pp. 1749–1751. https://jacow.org/e98/papers/TUP10G.pdf

[31] T. Kobayashi and K.Akai, "Advanced Simulation Study on Bunch Gap Transient Effect", Phys. Rev. Accel. Beams 19, 062001 (2016). https://link.aps.org/doi/10.1103/PhysRevAccelBeams.19.062001

[32] T. Kobayashi and K. Akai, "LLRF Controls Including Gap Transients at KEKB and Plans for SuperKEKB", in *Proc. eeFACT'16*, Daresbury, UK, Oct. 2016, pp. 177–184. doi:10.18429/JACoW-eeFACT2016-WET2H7